SIX PEAKS VISIBLE IN THE REDSHIFT DISTRIBUTION OF 46,400 SDSS QUASARS AGREE WITH THE PREFERRED REDSHIFTS PREDICTED BY THE DECREASING INTRINSIC REDSHIFT MODEL

M. B. BELL[1] AND D. McDIARMID[1]

ABSTRACT

The redshift distribution of all 46,400 quasars in the Sloan Digital Sky Survey (SDSS) Quasar Catalog, Third Data Release (DR3), is examined. Six peaks that fall within the redshift window below $z = 4$ are visible. Their positions agree with the preferred redshift values predicted by the decreasing intrinsic redshift (DIR) model. A power spectrum analysis of the full data set confirms the presence of a single significant power peak at the expected redshift period. Power peaks with the predicted period are also obtained when the upper and lower halves of the redshift distribution are examined separately. The periodicity detected is in linear z, as opposed to $\log(1 + z)$. Because the peaks in the SDSS quasar redshift distribution agree well with the preferred redshifts predicted by the intrinsic redshift relation, we conclude that this relation, and the peaks in the redshift distribution, likely both have the same origin, which may be intrinsic redshifts or a common selection effect. However, because of the way in which the intrinsic redshift relation was determined, it seems unlikely that one selection effect could have been responsible for both.

Subject headings: galaxies: active — galaxies: distances and redshifts — quasars: general

1. INTRODUCTION

Peaks in the distribution of quasar redshifts have been claimed as evidence for the existence of preferred redshifts, and a periodicity in $\log(1 + z)$ was suggested after only a few hundred redshifts were known (Karlsson 1971, 1977; Burbidge & Napier 2001). Since this claimed periodicity came from the early redshift samples themselves, until more complete samples became available, it was not possible to test it. Recently, using a SDSS quasar redshift sample containing approximately 5000 high-redshift quasars, it was demonstrated that there is little evidence that the previously claimed $\log(1 + z)$ periodicity fits the peaks in the SDSS redshift distribution above $z = 2$ (Bell 2004). However, it has been demonstrated that the redshift peaks found in the early data can be fitted reasonably well to a different intrinsic redshift relation that is quasi-periodic in linear redshift, as opposed to $\log(1 + z)$ (Bell 2002a, 2002c; Bell & Comeau 2003a). The intrinsic, or preferred, redshift components predicted in this model, z_{iQ}, are given by the relation

$$z_{iQ} = z_f[N - M_N], \tag{1}$$

where N is an integer, M_N is a function of a second quantum number n, defined previously (Bell 2002c; Bell & Comeau 2003a), and $z_f = 0.62 \pm 0.01$ is the intrinsic redshift constant. Unlike the $\log(1 + z)$ relation, this equation did not come from an analysis of peaks in a redshift distribution. It was determined instead after all Doppler components were estimated and removed from the redshifts of the 14 QSOs near NGC 1068 (Burbidge 1999; Bell 2002a, 2002b, 2002c). The intrinsic redshift components that led to equation (1) were obtained by fitting an ejection model to the sources. This model used both the measured redshifts and the distances of the sources from NGC 1068 to estimate ejection velocities before calculating the intrinsic redshift component.

All redshift components predicted by equation (1) are listed in Table 1 for values less than $z = 4.5$, and have been available in the literature for over 3 years. As can be seen from Table 1, equation (1) becomes periodic in $\Delta z = 0.62$ for $N > 4$. Below $N = 5$, each N-group contains additional redshift components that in all cases fall below the $z = 0.62N$ harmonic. Searching a quasar redshift distribution as large as that provided by the SDSS Third Data Release (DR3), for the preferred redshift values predicted by equation (1), represents *a completely independent test of this equation*.

Evidence was presented recently showing that peaks in the distribution of SDSS quasar redshifts near $z = 3.1$ and 3.7 had extended high-redshift wings that could be attributed to the presence of a small cosmological redshift component $z_c < 0.066$ (Bell 2004). Here the redshift distribution for 46,400 redshifts in the full SDSS DR3 sample (Schneider et al. 2005) is examined to see if there is evidence for a redshift periodicity that would be expected to result from the quasi-periodic preferred redshift values predicted by equation (1). First we carry out a power spectrum analysis on the entire SDSS redshift distribution, containing over 46,000 quasar redshifts. We then visually compare the SDSS redshift distribution to the quasi-periodic values predicted by equation (1) to demonstrate that the peaks found are in good agreement not only with the fundamental periodicity, but also with the subcomponents predicted by equation (1). We also obtain an independent estimate of the errors, and examine selection effects that might play a role in producing peaks in the distribution. Finally, we carry out spectral analyses on both the low- and high-redshift halves of the data.

2. OBSERVATIONS

If, as is assumed in the DIR model, quasars are ejected from active galaxies, and these galaxies are distributed uniformly in space, the same should be true for quasars, assuming that the ejection process is similar at all epochs. However, since in this model they are subluminous by several magnitudes when first born, distant, young quasars (QSOs) will not be detectable with current sensitivities. On the other hand, those with lower intrinsic redshifts, which are more luminous than those with high intrinsic

[1] Herzberg Institute of Astrophysics, National Research Council of Canada, 100 Sussex Drive, Ottawa, ON K1A 0R6, Canada; morley.bell@nrc.ca.

TABLE 1
Intrinsic Redshifts Predicted by Equation (1) for $z_{iQ} < 4.5$

(n)	$z_{iQ}[N=1,n]$	$z_{iQ}[N=2,n]$	$z_{iQ}[N=3,n]$	$z_{iQ}[N=4,n]$	$z_{iQ}[N=5,n]$	$z_{iQ}[N=6,n]$	$z_{iQ}[N=7,n]$
0..............	0.620	1.240	1.860	2.48	3.10	3.72	4.340
1..............	0.558	1.178	1.798	2.418	3.038	3.658	4.278
2..............	0.496	1.054	1.488	1.178			
3..............	0.434	0.868	0.558				
4..............	0.372	0.620					
5..............	0.310	0.310					
6..............	0.248						
7..............	0.186						
8..............	0.124						
9..............	0.062						

redshifts (Bell 2002a, 2002c), will be detectable to greater cosmological distances. It is also worth noting again that in the DIR model the intrinsic component present in quasar redshifts is superimposed on top of a second redshift component that has been found, at least in the local universe, to be indistinguishable from that of a Hubble flow with $H_0 = 58$ km s^{-1} Mpc^{-1} (Bell et al. 2004, and references therein).

In Figure 1, the histogram shows the distribution of 46,400 quasar redshifts from the SDSS Third Data Release (Schneider et al. 2005). The sources have been binned into redshift intervals with $\Delta z = 0.076$. The gross features in the redshift distribution, with a large, broad component below $z = 2.2$ and a low pedestal above $z = 2.4$, have resulted from data-selection effects. In the low-redshift source selection sample ($z < 2.2$), an i magnitude limit of 19.1 was imposed for candidates whose colors indicated a probable redshift of less than $\sim$3 (selected from the *ugri* color cube); in the high-redshift sample candidates (selected from the *griz* color cube) are accepted if $i < 20.2$. A detailed description of the quasar selection process and possible biases can be found in Richards et al. (2002). As can be seen from Schneider et al. (2005, their Figs. 2 and 4), (1) there are many more sources in the low-redshift sample than in the high-redshift sample, and (2) the upper cutoff of the low-redshift sample is abrupt. The broad

structure introduced by the low-redshift source selection process is expected to produce mainly long-period components in the power spectrum.

2.1. *Power Spectrum Analysis*

The power spectrum analysis of the entire data sample was carried out by taking a fast Fourier transform (FFT) of the histogram in Figure 1 for the 64 channels between $z = 0$ and 4.86. The power obtained is plotted versus redshift period as the solid curve in Figure 2, and versus frequency (z^{-1}) in Figure 3. In each case the negative values have been introduced by spline fitting. The vertical solid bar indicates 1 σ uncertainty estimated by Tang & Zhang (2005), who carried out a similar power spectrum analysis on the same data sample; it is taken from their Figure 9. The dotted curve represents this approximate 1 σ uncertainty plotted as a function of period and frequency, respectively. Estimating the uncertainty in power spectra can be a difficult process, and even when great care is taken the result needs to be treated with caution. As can be seen from Tang & Zhang (2005, their Fig. 1), the size of 1 σ increases with power, and caution must be
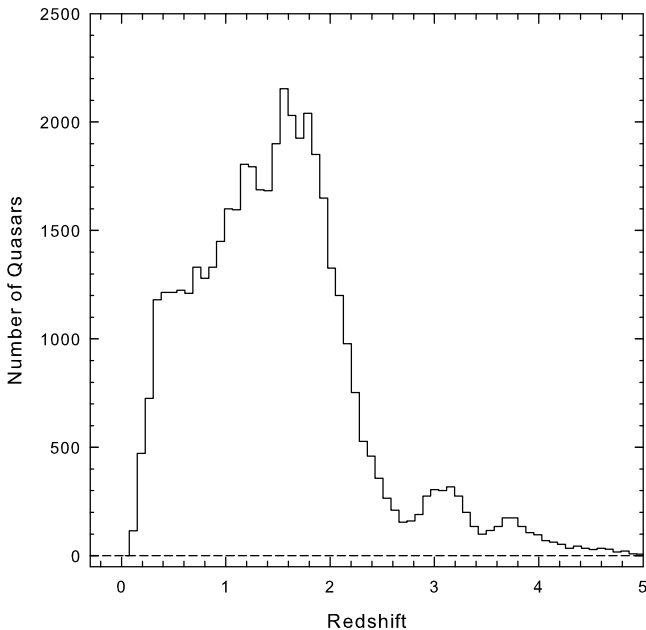

Fig. 1.—Distribution of 46,400 SDSS quasars with redshifts below $z = 5$ (Schneider et al. 2005).
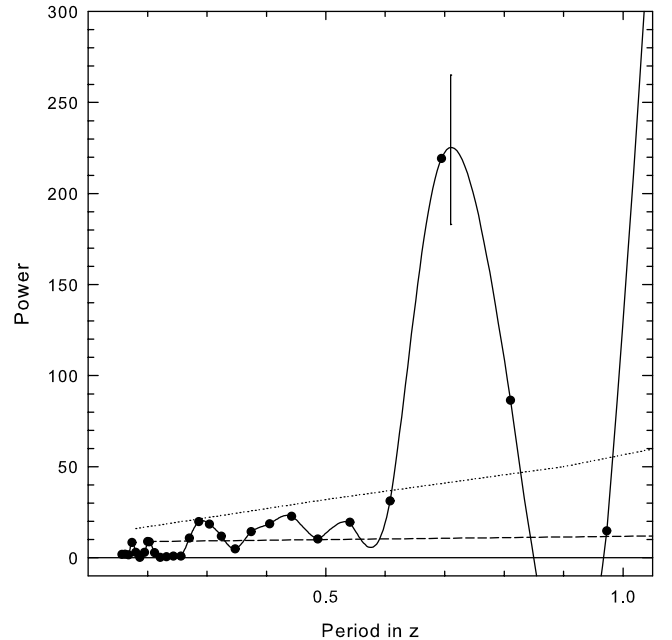

Fig. 2.—*Solid curve*: Spectral power obtained for over 46,000 quasar redshifts plotted vs. redshift period. The vertical bar and dotted line represent the 1 σ error taken from Tang & Zhang (2005). The dashed line represents the statistical uncertainty obtained for 46,000 randomly generated redshifts. Negative values are introduced by the spline fitting.
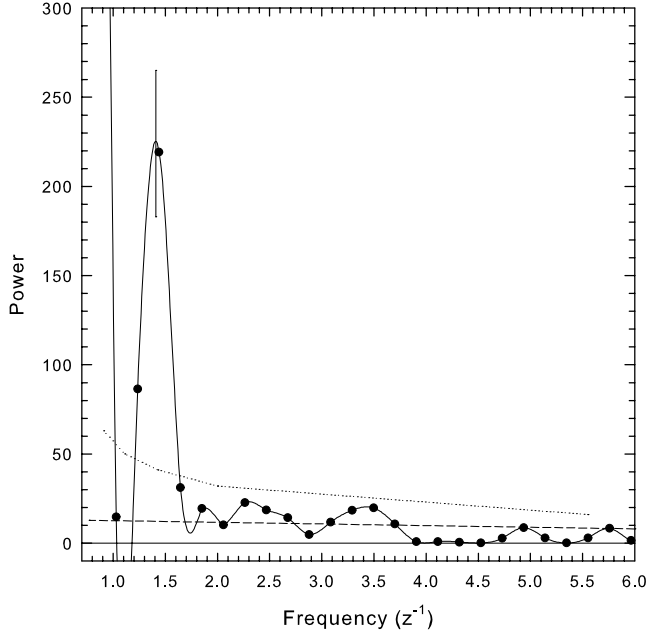
FIG. 3.—Spectral power distribution obtained for over 46,000 quasar red-shifts plotted vs. frequency (z^{-1}). See text for a description of the vertical bar. Dotted and dashed lines are as in Fig. 2.

taken if one attempts to use it to obtain a measure of the significance of the power peak. We independently determined the uncertainty that could be expected to be introduced by statistical fluctuations in the data when there are no selection effects present. To do this we generated three random sets of 46,000 redshifts, uniformly distributed between $z = 0$ and 4.86. The redshifts in each set were binned into 64 bins with a width of $\Delta z = 0.076$, exactly as was done for the real data. A power spectrum was then obtained for each of the three data sets, and the results are plotted in Figure 4 on an expanded power scale where the peak level

(dashed line) can be compared to the 1 σ value obtained by Tang & Zhang (2005) (dotted line). Our error represents the peak error that is produced by random, uniformly distributed fluctuations in a sample of 46,000 redshifts, plotted as a function of the harmonic number. This error level is significantly lower than the error set by Tang & Zhang (2005), and is plotted as a dashed line in Figures 2, 3, and 4.

Tang & Zhang (2005) found, as we do, that there is a significant periodicity with period near 0.7 in redshift in the full sample containing over 46,000 redshifts; regardless of which error estimate is used, the question that now needs to be answered is whether this power peak is due to the presence of preferred redshifts or to selection effects.

The strong power level above $\Delta z \sim 1$ arises almost entirely from the shape of the distribution created by the low-redshift data selection effect discussed above.

3. COMPARISON BETWEEN THE DATA PEAKS AND THE PREDICTED PREFERRED REDSHIFTS

Above, we found that there was a significant power peak in the redshift distribution with a period near $\Delta z = 0.7$. Equation (1) predicts preferred redshifts that are quasi-periodic, with a slightly shorter period of $\Delta z = 0.62$. Here we examine the redshift distribution together with the redshifts predicted by equation (1) to see whether this difference can be explained. Although several peaks are already visible in the raw redshift distribution in Figure 1, before undertaking this comparison it is first helpful to remove the broad, smooth baseline component below $z = 2.4$, on top of which the peaks are superimposed. We did this using two different techniques, and the results are shown in Figure 5. First we subtracted a smooth, low-redshift baseline curve. The curve used is shown by the smooth curve in Figure 6, and its shape, with a relatively sharp upper cutoff, is based on the shape of the number versus magnitude distribution produced by the
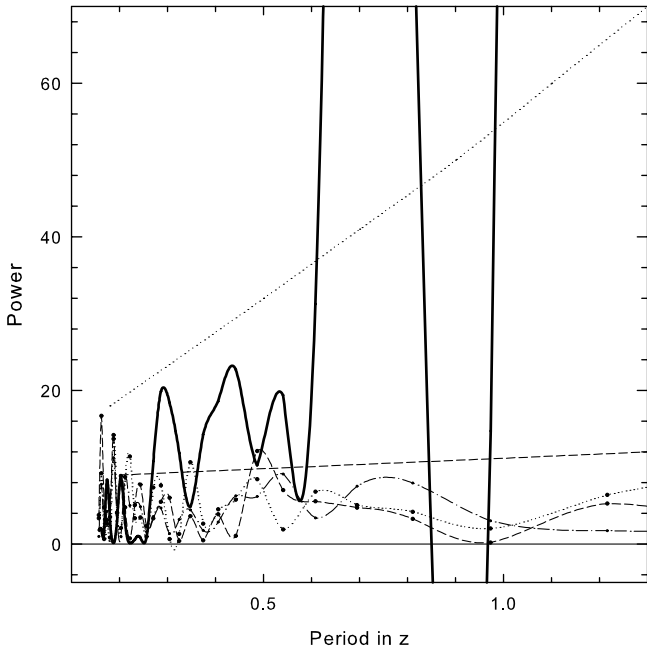

FIG. 4.—Solid curve: FFT of the distribution 46,400 SDSS redshifts. Dashed, dotted and dashed-dot curves: FFTs of 46,000 randomly generated redshifts. Dashed and dotted straight lines: uncertainties as in Figs. 2 and 3.
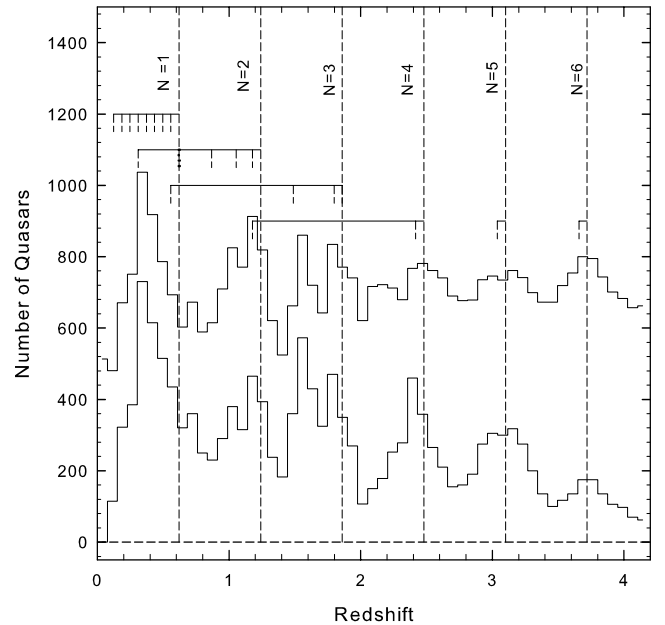

FIG. 5.—Lower histogram: Distribution of SDSS quasar redshifts after removal of the curved baseline in Fig. 6. Upper histogram: Distribution of quasar redshifts obtained after taking the Fourier transform, setting the first four non-DC Fourier components to zero, and then taking the inverse Fourier transform. The vertical dashed lines indicate the positions of the highest redshift in each N-group from eq. (1). The vertical short-dashed lines indicate redshifts from eq. (1) that fall below the maximum in each N-group.
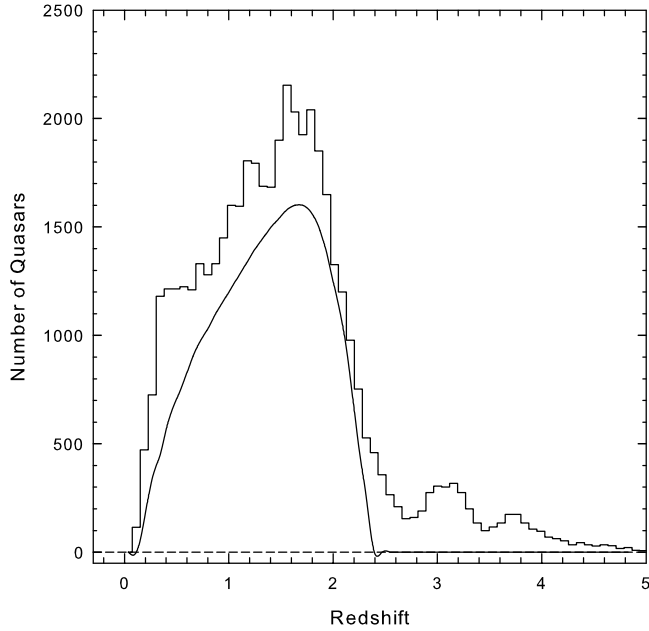
Fig. 6.—*Upper histogram*: Distribution of 46,400 SDSS quasars with redshifts below $z = 5$ (Schneider et al. 2005). See text for a description of the curved baseline below $z = 2.4$.

low-redshift subsample (Schneider et al. 2005; their Fig. 4), and the fact that there is a relation between redshift and magnitude. In the DIR model this broad, featureless curve is attributed to sources whose cosmological expansion, or Doppler ejection, redshift components are comparable to, or larger than, the spacing between the predicted intrinsic values. The resulting redshift distribution curve, after subtraction of the smooth baseline curve, is shown by the lower curve in Figure 5. However, because the shape of this smooth baseline curve is somewhat arbitrary, it is conceivable that its removal may have introduced some spurious features. This is especially true near $z = 2.5$, where the curve ends abruptly. Therefore, we also used a second, more objective method to remove the broad low-redshift selection effect. In this method, after obtaining the Fourier components for the entire sample, the first four non-DC Fourier components were then set to zero. This effectively filters out all long-period fluctuations. The inverse Fourier transform was then obtained, and the result is plotted in the upper curve in Figure 5. Both techniques gave similar results, and six peaks between $z = 0$ and 4 are clearly visible in each curve. In Figure 5, the vertical dashed lines indicate the positions of the highest redshift in each N-group as defined by equation (1). The shorter dashed lines indicate the positions of the lower redshift subcomponents in each N-group. Since these components are predominantly present in only the first three N-groups, and all lie at lower redshifts, this will introduce an effective stretching out of the peak separation at the low-redshift end of the distribution. This effect is most clearly visible in the first N-group, where the peak is centered near the mean $N = 1$ group redshift of $z = 0.31$.

In addition to this stretching at the low-redshift end of the distribution, if there is a small cosmological component present, as argued previously (Bell 2004), this will also tend to stretch out the high-redshift end of the distribution. Using the relation $(1 + z) = (1 + z_c)(1 + z_i)$, where z_c is the cosmological component and z_i is the intrinsic one, for a mean cosmological component of $z_c = 0.02$ the intrinsic redshift peak at $z_i = 3.72$ would be stretched to $z = 3.81$. It is therefore possible to obtain a rough

estimate of how significant the total stretching effect will be when the redshifts predicted from equation (1), together with the stretching at both the low and high ends of the distribution, are taken into account. Since there are five N-cycles between $z = 0.31$ and 3.81, a period of $\Delta z = 0.70$ is estimated from Figure 5, for a mean cosmological redshift of $z_c = 0.02$. This period agrees well with the power peak obtained. Close examination of Figure 5 reveals that not only are there peaks associated with all harmonics of 0.62 below $z = 4$, but there is also reasonable agreement below $z = 2$ with the predicted redshift subcomponents. For example, the peaks at 0.31 and 1.1 coincide with regions where there is a high density of preferred redshift components. Also, the double peaks at $z = 1.55$ and 1.85 agree well with the predicted preferred redshifts of 1.488 and 1.798, if a small cosmological component is present.

4. SPECTRAL ANALYSIS OF THE UPPER AND LOWER HALVES OF THE REDSHIFT DISTRIBUTION

Because the detection efficiency of the SDSS is lower near $z = 2.7$ and 3.5, this could have contributed to the depth of the valleys seen in the redshift distribution at these redshifts (Schneider et al. 2005). It is therefore of interest to see whether there is a contribution to the observed power peak that comes solely from the lower half of the redshift distribution ($z < 2.4$), keeping in mind that, because the density of lines predicted by equation (1) is higher in this redshift range, preferred redshifts will be more easily smeared out if small cosmological redshift components are present.

Figure 7 shows power spectra obtained by splitting the redshift range into two halves. The spectrum of the lower half of the redshift range (32 bins below $z = 2.4$) is shown by the solid line, and that of the upper half by the dashed line. Because only half of the redshift range has been covered here, the spectral resolution is reduced. Because of this, the strong low-frequency components present in the low-redshift half of the data make it impossible to completely resolve the peak near $z^{-1} = 1.5$. Although there is evidence for an unresolved feature in the solid curve in Figure 7, it will be necessary to remove the low-frequency components
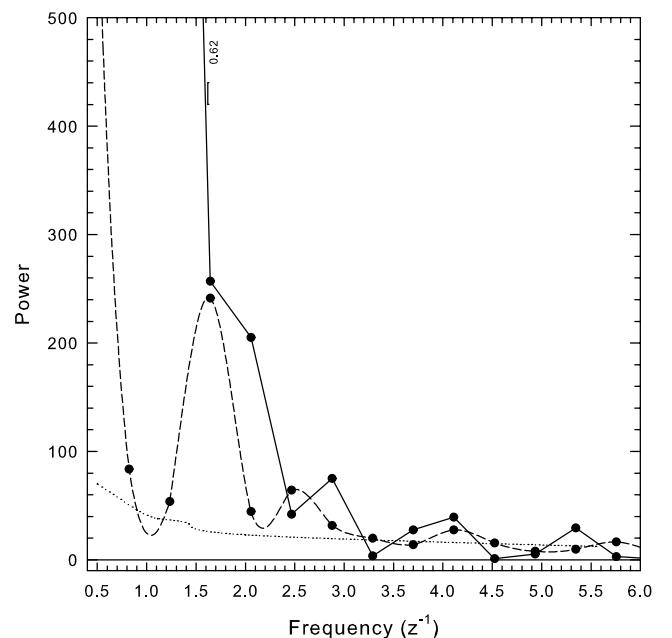

Fig. 7.—FFT of bottom 32 bins (*solid line*) and upper 32 bins (*dashed line*) of the redshift range.
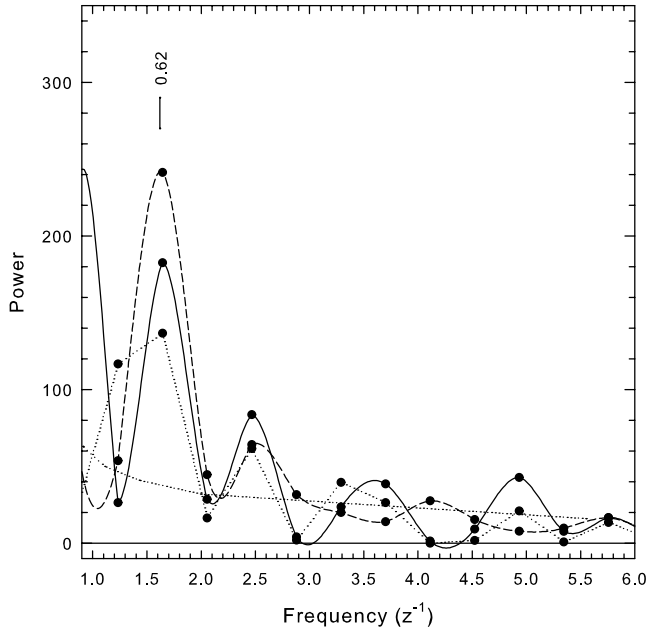
FIG. 8.—Power vs. frequency. *Dashed line*: Upper half of redshifts; *solid line*: lower half of redshifts after smooth baseline has been removed. *Dotted line*: Lower half of redshifts with first four harmonics removed.

FIG. 9.—Spectral power vs. frequency for 32 bins above $z = 2.0$ (*solid curve*) and 32 bins above $z = 2.4$ (*dashed curve*).

before a convincing power peak can be resolved. To do this, we removed the low-frequency Fourier components as was done for the curves in Figure 5, and recalculated the FFT. In Figure 8 the results are again compared to the power spectrum obtained for the upper half of the redshifts. Here the solid curve was obtained using the lower curve in Figure 5, and the dotted curve corresponds to the upper curve. There is now clear evidence for a power peak near a frequency of 1.6 in the lower half of the redshift data in Figure 8. Tang & Zhang (2005) did not correct for the effects of strong low-frequency components when they examined the lower half of the redshift data and would not have been able to detect this feature. They also did not detect a significant power peak near $\Delta z = 0.62$ in the high-redshift sample because they extended the redshift range down to $z = 2$, which covers a portion of the much more highly populated low-redshift source sample. This caused them to include the large transition step between the two redshift samples that is produced solely by this selection effect. This would likely strongly affect the transform. The resulting strong, longer period power peak near 0.75 introduced by the portion of the redshift distribution between $z = 2$ and 2.4 (see their Fig. 11d) appears to have overwhelmed the peak at $\Delta z = 0.62$, and prevented its detection. We demonstrate this in Figure 9, where the solid line represents the spectral power obtained for 32 bins above $z = 2$. The dashed line represents the power spectrum obtained for 32 bins above $z = 2.4$. There is no evidence for a power peak at $\Delta z = 0.62$ in the former, but one is clearly visible in the latter.

The strong peak in the upper half of the data shown by a dashed line in Figures 7 and 8 has a period P of $\Delta z = 0.62$. That this period, over a redshift range where few subcomponents are present, is exactly equal to the harmonic constant z_f, is further evidence that the valleys near $z = 2.7$ and 3.5 may *not* be caused entirely by the suggested selection effect; this is discussed further in the next section.

It is also worth noting that when periodicities are sought in the low-redshift half of the data, this transition step between $z = 2$ and 2.4 also plays a role in preventing detection of the period
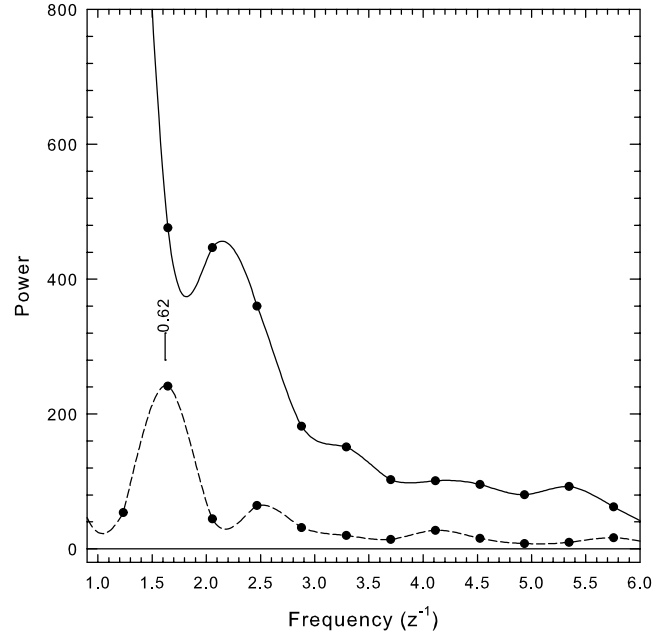
being sought. When a power spectrum is obtained for the redshift range from $z = 0$ to 2, a significant power peak near the expected frequency is obtained immediately, without any further need to remove low-frequency components.

5. SELECTION EFFECTS IN THE DATA

Just because there appears to be good agreement between the peaks in the redshift distribution and the preferred redshifts predicted by equation (1), this does not necessarily mean that intrinsic redshifts are real. As mentioned above, there are selection effects that have been claimed to explain the valleys in the distribution near $z = 2.7$ and 3.5, and there could conceivably also be other selection effects responsible for the other valleys in the distribution. Because quasar colors are similar to those of stars at redshifts near $z = 2.7$ and 3.5, finding all the quasars at these redshifts would be a formidable task, since it would require measuring the redshifts of all the stars as well. The strategy used to avoid this could have resulted in the valleys at these redshifts. However, we also point out that equation (1) predicts that no quasars will have these preferred redshift values, except for a few that have been shifted there because they also have a large cosmological component or a large ejection velocity component, or both. In this case the suggested selection effect could not play a significant role. If there are few sources there, finding only a small fraction of them would not change the result, and even if all sources were examined, no quasars would be found. The only way to prove that the suggested selection effect is causing the dips is then to measure every object with these colors. Until this happens, the correct explanation of these dips will remain unknown.

However, there may be other evidence to indicate that the suggested selection effect is not the only explanation for the high-redshift valleys. In Figure 10 the high-redshift portion of the distribution has been replotted. The valleys near $z \sim 2.7$ and ~ 3.5 have similar widths, with depths that are approximately 50% of the peaks estimated by the dashed line. However, Figure 10 of Richards et al. (2002) shows that the dip at $z \sim 3.5$ should be much narrower and shallower than the one at $z \sim 2.7$. The hatched areas in Figure 10 show the regions where the
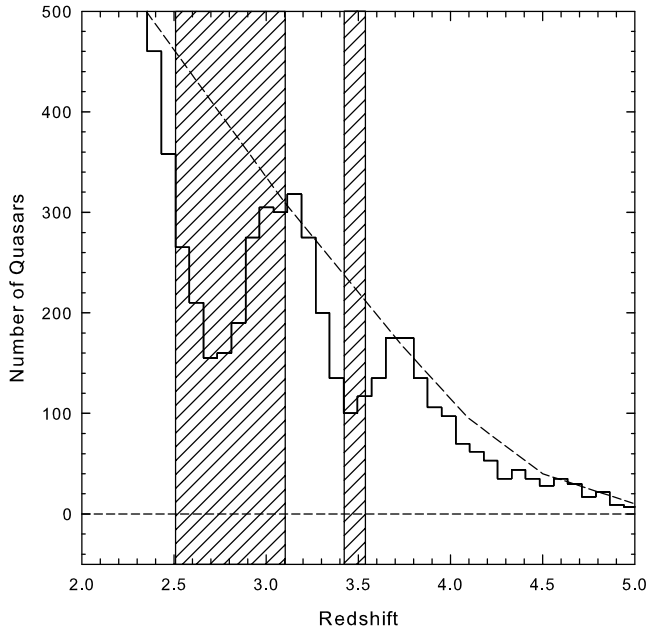
Fig. 10.—Cross-hatched areas show the regions in which valleys are expected to appear from Richards et al. (2002, Fig. 10). See text for further comments.

Fig. 11.—*Solid oblique lines*: Relation between redshift and observed wavelengths for strong emission lines. *Dashed lines*: Wavelengths of gaps between SDSS filters. *Solid vertical lines*: Locations of valleys in the redshift distribution. *Dotted lines*: Locations of peaks in the distribution. The filter designation is given along the right edge.

valleys are expected, and there is poor width agreement for the valley at $z \sim 3.5$. Also, from Richards et al. (2002, Fig. 10) this dip appears to be much deeper, relative to the one at $z = 2.7$, than would be expected if it were due to the suggested selection effect.

It has also been suggested that optical observing effects, such as strong emission lines redshifting through the observing window, and the availability of search lines at certain redshifts, etc., could result in sources being more easily detected at certain redshifts (Basu 2005, and references therein). Since the quasars in the SDSS sample are identified optically, the redshift distribution could conceivably have been influenced by these kinds of optical selection effects, if they are significant. In Figure 11 the relation between redshift and the observed wavelengths of the strong emission lines is shown. Here the horizontal dashed lines represent the locations of the gaps between the SDSS filters (Richards et al. 2002; their Fig. 4). It is easily seen at which redshifts the strong lines are located inside each filter passband. Included in the figure are vertical dotted lines representing the locations of the peaks found in the redshift distribution. The locations of the valleys are indicated by the vertical solid lines. There are several observations that can be made concerning this plot. First, the peak at $z \sim 0.3$ occurs at a redshift that places the strong hydrogen Balmer lines (Hα and Hβ) in the gaps between filters. This is contrary to what would be expected if these lines were influencing the source selection at this redshift. Second, the valley near $z = 0.8$ occurs when the Mg II and Hβ lines are in the g and i filter passbands, respectively, again contrary to what would be expected if these line were influencing the source selection. There are other examples, some that agree and some that disagree, but there appears to be little correlation between the presence of these strong lines in the filter passbands, and the presence of peaks in the redshift distribution.

Over the past 35 years many attempts have been made to attribute features in the redshift distribution to optical selection effects (Karlsson 1971; 1973; Roeder 1971; Lake & Roeder 1972; Box & Roeder 1984; Kjaergaard 1978; Burbidge & Napier 2001; Bajan et al. 2003, 2004; Basu 2005). During this period,
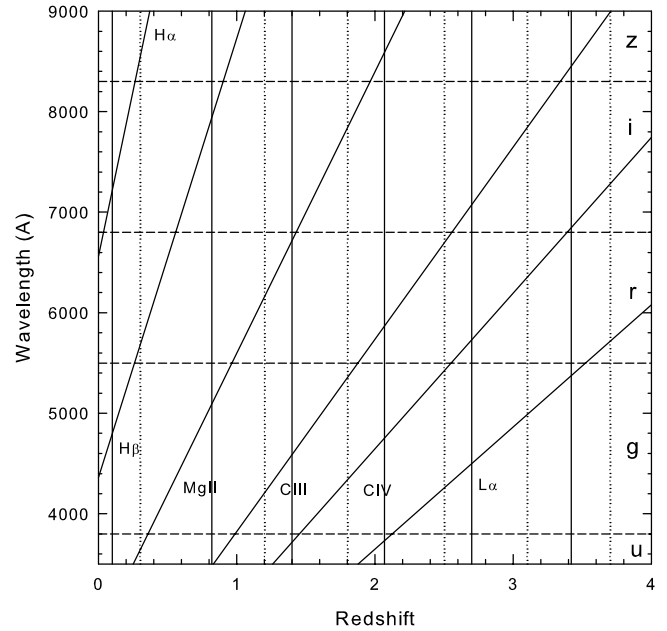
the peak locations have changed above $z = 2$, so some of the previously claimed peak/selection effect correlations are no longer valid. Furthermore, observing methods have also changed (different filters used, etc.), but the peaks that were found to agree even with the redshift subcomponents predicted by equation (1) remain (Bell 2002c; Bell & Comeau 2003b). This is a strong argument that selection effects related to optical emission lines are not the cause of these peaks. Although Roeder (1971) claimed that broad peaks near $z = 0.3$ and $z = 2$ were due to the presence of strong lines in the observing window, when the number of available lines are plotted as a function of redshift the distribution produces only long period Fourier components. No power is seen at $P = 0.7$, although this could conceivably change with the addition of a few more sources at the appropriate locations, since the numbers involved were so small. This is not the case here, however, with 46,000 redshifts.

Tang & Zhang (2005) report no evidence for a periodicity in the quasar redshift distribution obtained in the Two Degree Field QSO Redshift (2QZ) survey. It is also readily apparent when the number of 2QZ quasars is plotted versus redshift (Croom et al. 2004; their Fig. 3) that the peaks visible in the SDSS redshift distribution are not visible in the 2QZ distribution. We now have to ask, why? When two independent surveys are obtained using optical identification techniques, if the peaks seen in one are due to optical selection effects, why do these selection effects not produce peaks in the other? Even if different filters are used the peaks should be present at some other redshift. This result suggests that optical selection effects are not the source of the peaks in the SDSS distribution. However, if the peaks are real, their absence in the 2QZ distribution must still be explained. Tang & Zhang (2005) explained this result by arguing that the 2QZ sample is more complete, and therefore less affected by selection effects. This argument is not valid in our opinion. In what sense is it more complete, especially below $z = 2.4$, and how does this completeness avoid the optical selection effects? Their argument is meaningful only if the valleys below $z = 2.4$ in the SDSS

distribution are produced by the same type of selection effect as was suggested to explain the valleys at $z = 2.7$ and $z = 3.5$. However, this is unlikely, and to the best of our knowledge it has not been suggested in SDSS publications.

That there is little evidence for a period in the 2QZ redshift distribution can be explained if that survey found more sources with larger cosmological components present in their measured redshifts, filling in the valleys and smearing out the peaks. The aim of the 2QZ Survey was to measure redshifts for 25,000 optically-selected QSOs with $b_J < 20.85$ and $z < 3$ (Croom et al. 2004). As noted above, the SDSS i-band limit was <19.1, and thus the 2QZ survey may have detected sources with larger cosmological components, although how big this effect might be is difficult to determine. This could have smeared out peaks in the 2QZ distribution, especially below $z = 2.4$, where the density of intrinsic components is higher. This is not an unrealistic conclusion, since the broad baseline in Figure 6 is assumed to represent many sources in the SDSS sample that have cosmological, or Doppler ejection, components sufficiently large to smear out at least a portion of the peaks. The 2QZ survey was not designed to detect sources above $z = 3$, so it cannot be used to form any conclusions about the valleys that appear near $z = 2.7$ and 3.5 in the SDSS distribution.

6. DISCUSSION

Recently, Tang & Zhang (2005) used a quasar-galaxy pairing analysis to investigate the question of whether or not high-redshift quasars are likely to be born through ejection from a parent active galaxy. It is difficult to assess the significance of this approach in finding parent galaxies, since the required assumptions are rather poorly known.

The Tang & Zhang (2005) analysis could thus have missed, or misidentified, many of the parent galaxies, which could explain why the pairs they found differed little from what would be expected for a random distribution. Actually, their pairs do show a slight excess near the expected value of 200 kpc (see their Fig. 7). That result is reproduced here in Figure 12, which represents their "true pair" plot with their random galaxy curve subtracted from it. A typical projected separation value near 200 kpc was reported previously (Burbidge & Napier 2001; Burbidge 2003). If the objects are ejected uniformly in all directions, a higher number would be seen when they are ejected closer to the plane of the sky. Although Tang & Zhang (2005) concluded that QSOs are not ejected from active galaxies, in our opinion it is unlikely that their pair-finding technique could produce results with significance approaching those of previous researchers (see Burbidge 1996, and references therein for a review), whose parent galaxy claims have been simultaneously backed up by other independent observations. As an example, we refer here to the case of the high-redshift QSO in front of the galaxy NGC 7319 (Galianni et al. 2005).

Here we have examined data samples containing (1) the entire SDSS redshift distribution with 46,400 sources, (2) the bottom half of that distribution containing approximately 40,000 sources, and (3) the upper half of that distribution containing approximately 6000 sources. All three showed evidence for the period predicted by equation (1). It is also worth noting that a fourth source sample containing the 574 quasar redshifts used by Karlsson (1971, 1977) was examined previously (Bell 2002c; Bell & Comeau 2003b), and it was found that the peaks in that distribution also correlated well with the preferred redshifts predicted by equation (1).

One of the most important aspects of the SDSS data has to be the huge number of sources involved. We conclude here that the
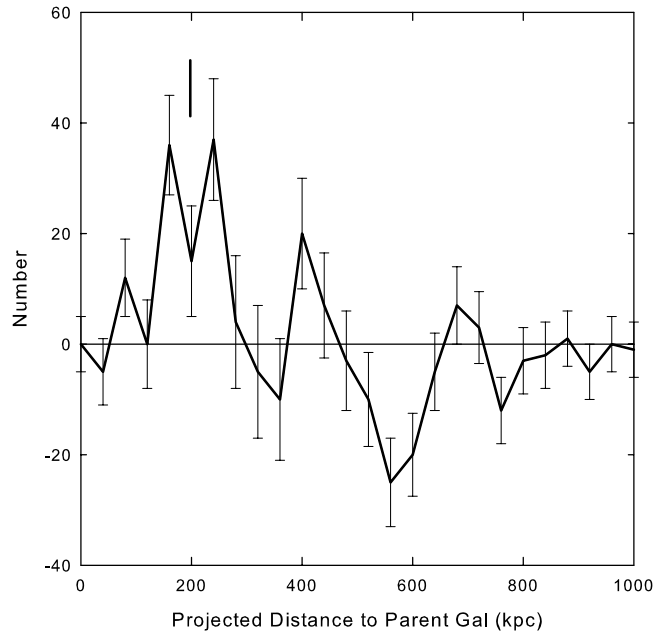

Fig. 12.—Difference between "true pairs" curve and randomly distributed galaxy curve taken from Tang & Zhang (2005, Fig. 7). The vertical bar indicates that there is a slight excess of sources near 200 kpc, the separation found by others to be typical for ejected sources. Error bars have been taken from Tang & Zhang (2005).

significant power peak found for the full SDSS redshift distribution, with a period near $\Delta z \sim 0.7$, is real (i.e., not a statistical fluctuation), and is due to either selection effects in the data or the presence of preferred redshifts. Because of the good agreement we find between the observed peaks and the preferred redshifts predicted by equation (1), it would seem likely that they have a common origin, and whatever that is, it must be able to explain both. This equation was derived empirically several years ago using a completely independent set of redshifts that were obtained by measuring the redshifts of X-ray excess QSOs near NGC 1068. The intrinsic redshift components were derived after removal of all ejection-related Doppler components, some of which produced redshift components as large as 0.366 (Bell 2002c), which came from an ejection model (Bell 2002a, 2002b) that was based on the source positions on the sky relative to NGC 1068. *As a result, it is very unlikely that a common selection effect could have been involved*. This may rule out selection effects as the common origin of the peaks in the SDSS redshift distribution and the preferred values predicted by equation (1).

7. CONCLUSIONS

A power spectrum analysis of the distribution of over 46,000 SDSS quasar redshifts has been found to show a single, distinct power peak for redshift periods less than $\Delta z = 1$. The peak found corresponds to a redshift period of $\Delta z \sim 0.70$. Not only is a distinct power peak observed, but the locations of the peaks in the redshift distribution are in agreement with the preferred redshifts predicted by the intrinsic redshift equation (eq. [1]). The power peak is detected in three different samples: the full SDSS sample, and the the lower and upper halves of the redshift distribution. We conclude that it is real, and is due to either the preferred redshifts predicted in the DIR model, or selection effects. However, because of the way in which the intrinsic redshift relation was determined, it seems unlikely that one selection effect could have been responsible for both.

REFERENCES

Arp, H., Fulton, C., & Roscoe, D. 2005, preprint (astro-ph/0501090)
Bajan, K., Flin, P., Godlowski, W., & Pervushin, V. N. 2004, Phys. Part. Nuclei, 35, 178
Bajan, K., et al. 2003, Spacetime & Substance, 4, 225
Basu, D. 2005, ApJ, 618, L71
Bell, M. B. 2002a, ApJ, 566, 705
———. 2002b, ApJ, 567, 801
———. 2002c, preprint (astro-ph/0208320)
———. 2004, ApJ, 616, 738
Bell, M. B., & Comeau, S. P. 2003a, preprint (astro-ph/0305060)
———. 2003b, preprint (astro-ph/0306042)
Bell, M. B., Comeau, S. P., & Russell, D. G. 2004, preprint (astro-ph/0407591)
Box, T. C., & Roeder, R. C. 1984, A&A, 134, 234
Burbidge, E. M. 1999, ApJ, 511, L9
Burbidge, G. 1996, A&A, 309, 9

Burbidge, G. 2003, ApJ, 585, 112
Burbidge, G., & Napier, W. M. 2001, AJ, 121, 21
Croom et al. 2004, MNRAS, 349, 1397
Galianni, P., Burbidge, E. M., Arp, H., Junkkarinen, V., Burbidge, G., & Zibetti, S. 2005, ApJ, 620, 88
Karlsson, K. G. 1971, A&A, 13, 333
———. 1973, Nature Phys. Sci., 245, 68
———. 1977, A&A, 58, 237
Kjaergaard, P. 1978, Phys. Scr., 17, 347
Lake, R. G., & Roeder, R. C. 1972, JRASC, 66, 111
Richards, G. T., et al. 2002, AJ, 123, 2945
Roeder, R. C. 1971, Nature Phys. Sci., 233, 74
Schneider et al. 2005, AJ, 130, 367
Tang, S. M., & Zhang, S. N. 2005, ApJ, 633, 41